

Irradiation of low energy ions damage analysis on multilayers

M.G. Sertsu^{1,2,4*}, A.Giglia³, L.Juschkin⁴, P. Nicolosi^{1,2}

¹University of Padova, department of Information Engineering, via Gradenigo 6B, 35131 Padova, Italy

²Consiglio Nazionale delle Ricerche-Institute for Photonics and Nanotechnologies Laboratory for Ultraviolet and X-ray Optical Research, via Trasea 7, 35131, Padova, Italy

³CNR- Istituto Officina Materiali, I-34149 Trieste, Italy

⁴RWTH Aachen University, Experimental Physics of Extreme Ultraviolet, Steinbachstr 15, 52074 Aachen, Germany

ABSTRACT

Impacts of low energy He⁺ ions on reflectivity and stability of EUV multilayers is investigated in this work. Combination of X-ray reflectivity, grazing incidence EUV reflectivity near Silicon edge, and theoretical ion irradiation damage analysis can explain the degradation of ML performances. It is found that MLs irradiation of 4 keV helium ions degrades reflectivity performances with much more impact on grazing incidence mirrors. The proposed method can also regain changes in optical properties due to the irradiations of low energy ions.

Keywords: Ion damage of multilayers, EUV multilayers, grazing incidence EUV, TRIM damage vacancies, X-ray reflectivity, EUV reflectivity, Synchrotron measurement

1. INTRODUCTION

Efforts to study the sun and its solar system have been dramatically growing over the last two decades. A number of solar mission satellites throughout the world have been under strict preparation in order to study the sun's atmosphere in an ever-closest distance [1]. Major ones such as the European Solar Orbiter mission aims to answer high significance scientific questions regarding the sun-heliosphere connection [2]. Solar Orbiter, the first mission of ESA's Cosmic Vision 2015 - 2025 program, is expected to address how the sun creates and controls the heliosphere.

Several imaging and spectroscopic devices have been part of the payload in any solar mission to produce images of solar transition region that extends from the chromosphere up to solar corona. This outer surface of the sun (i.e. the solar corona) contains mostly hot plasma that radiates EUV and X-ray wavelengths, due its high temperature, according to the blackbody radiation principle [3, 4]. An imaging package in the EUV and soft X-ray regime, that mainly contain multilayers for collecting radiation through reflection and focusing onto the CCD, can give more information about the contents of sun's outer region. Famous missions with multilayers (MLs) included in the imaging payload are the SOLO (Solar orbiter) and SOHO (Solar and Heliosphere Observatory) missions [5, 6].

However, the sun's environment is not friendly to optical components on board. Low energy particles such as protons and α -particles from solar wind plasma, thermal loads, continuous irradiations, and natural aging processes affect the performances of optical devices in general and multilayers in particular. Thus, detail study of the MLs before they make it on board to any solar missions is indispensable.

Previous studies in [7-9] have experimentally demonstrated degradation of near normal reflectivity performances, structural damage on top layer and roughening of Si/Mo MLs after exposed to doses of protons and alpha-particles. Further studies on how the radiation from sun affects MLs in relation to thermal and radiation stabilities, structural and optical damages, and performance changes in time are still expected.

In this piece of work, a combination of experimental and numerical methods is implemented to perform analysis of optical and structural changes of MLs due to low energy ions irradiation damage. In addition to a physical damage observed on the top few layers, cascaded damages such as vacancies, interstitials, and atomic displacements at each layer

are simulated and their impacts on EUV reflectivities are studied. Comparison of several experimental results of two MLs of same kind, one exposed to low energy ions and the other non-exposed, is expected to differentiate impacts of energetic ions on performance, optical and structural properties of MLs.

2. SAMPLE DESCRIPTION, EXPERIMENT AND DATA PROCESSING

Prototype MLs have been deposited at Reflective X-Ray Optics LLC (New York, USA) by DC magnetron sputtering onto polished Si (100) substrates. The MLs were design to reflect at 5° incidence angle from normal based on early requirements for Multi Element Telescope for Imaging and Spectroscopy (METIS) coronagraph [5, 6]. They are designed and optimized to simultaneously image in visible light between 450 and 650 nm, hydrogen Lyman- α line at 121.6 nm and He-II Lyman- α line at 30.4 nm [6].

A total of four Si/Mo ML samples with protective capping structures are studied in this paper. Two of the MLs are over coated with a pair of Si-Mo capping layers (CL1), and the other two are capped with Ir-Mo (CL2) pair. One sample from each pair is exposed to low energy helium ions (He+) of 4 keV energy, while the other pair is kept unexposed for a reference purposes. Capping structures are given in Table 1.

The interior ML samples (excluding capping structures) consist of Si/Mo periodic structures on Si Substrate that are designed to have a period $d= 16.4\text{nm}$, thickness ratio $\Gamma =0.82$, $t_{\text{Si}} = 13.45\text{nm}$, $t_{\text{Mo}} = 2.95\text{nm}$ and number of periods $N=25$. Γ – ratio in this work refers to thickness ratio of spacer layer (Si) to period of the ML.

Table 1: ML capping layers (CL). CL1 refers to Si/Mo and CL2 is Ir/Mo capping structures.

ML capping layer structures	
CL1	CL2
Si (187.2 Å)	Ir (20 Å)
Mo (35 Å)	Mo (22 Å)

Two of the ML coatings (one with CL1 and another with CL2) were exposed to a flux of low energy He+ particles (4 keV) based on a dose fluency expected in SOLO mission environment. Alpha-particle doses are derived from data of solar irradiation at 1AU [10] with appropriate scaling to the varying distance at each point of the orbit from the sun, and finally integrated over a time of 4 years ($\approx 2.6 \times 10^{15}$ ions/cm²) which is expected time length the SOLO satellite will stay around the sun atmosphere. Sample irradiation to He+ ions were performed at the low energy implanter facility, Institute of Ion-beam Physics and Materials Research, HZDR, Dresden (Fig 1).



Figure 1: Low energy ion (LEI) facility at Forschungszentrum Dresden-Rossendorf with open sample holder (right)

Several measurements have been performed to derive damage information of exposed MLs. At-wavelength grazing incidence EUV reflectivity (GI-EUVR) measurements near Si-L_{III} edge were carried out at the BEAR (Bending magnet for Emission, Absorption and Reflectivity) beam line, ELETTRA Synchrotron in Trieste [11] using nearly linearly s-polarized incidence beam (> 90% polarization). Measurements have been performed near the Si L-edge resonance radiation at about 99 eV. Higher order rejection was accomplished by using a 0.1μm thick Si filter. The stability and reproducibility of the synchrotron source, working in top-up mode, the monitoring setup of the incoming beam intensity and the high control of the beam-line experimental setup, allowed to get reliable experimental data with a SNR of 0.5%. This innovative GI-EUVR method of ML analysis is expected to extract damage information throughout the ML depth in addition to what has been studied with a near normal EUV reflectivity [9].

On the other hand, X-ray reflectivity (XRR) measurements have been done at Cu K_α line (8047 eV) with accelerated voltage and current of 40 kV and 40 mA respectively in 2θ – ω scan of the X'PERT-PRO diffractometer system [12] at the Physics department in Padova. All the four ML samples were measured in both XRR and GI-EUVR experiments with same experimental set up and incidence beam properties.

Measured data (XRR, GI-EUVR) and a nonlinear least square curve fitting to them via a robust genetic algorithm (GA) optimization is a primary analysis method implemented. Multilayer ion irradiation damage analysis software to extract relevant structural and optical changes at exposure to low energy helium ions vis-à-vis a non-exposed (reference) sample. GI-EUVR near the resonance edge of Si enables to reconstruct optical constants of interlayers that might be formed due to diffusion, derive any drift in optical constants in any of the layers (e.g. Si layers), and determine interlayer thicknesses by trying to fit to the measured Bragg peaks in EUV [13]. XRR measurements have dual merit in this analysis. One is to show if interlayers are formed or not during deposition of MLs by comparing design and measured values of Γ-ratios. A significant change of Γ – ratio from a design value is a typical indication of interlayer formation as the modulation of intensity of Bragg peaks depend on it [14]. Second, a nonlinear least square curve fitting in IMD software to the measured XRR helps to derive ML period and layer thicknesses. The high depth resolution of XRR due to its short wavelength (1.54 Å) enables to capture period (d) and Γ changes that can happen during exposure to low energy ions [15].

At last, damage analysis of MLs due to irradiation of low energy He+ ions in TRIM (Transport of Ions in Medium) simulation software is performed. TRIM is a comprehensive program which calculates the stopping range of ions (up to 2 GeV/amu) into matter using quantum mechanical treatment of ion-atom collisions (assuming a moving atom as an "ion", and all target atoms as "atoms") [16-18].

3. RESULTS AND DISCUSSION

As mentioned above, ion irradiated sample (irr) is analyzed in contrast with its reference (REF) sample. Measured data of XRR and GI-EUVR for both exposed (irr) and non-exposed (REF) MLs, both with CL1 are plotted in Fig 2. The fact that exposed and non-exposed sample pairs were deposited at same time and passed through same deposition and measurement conditions enable to systematically bypass the issue of aging and measurement errors.

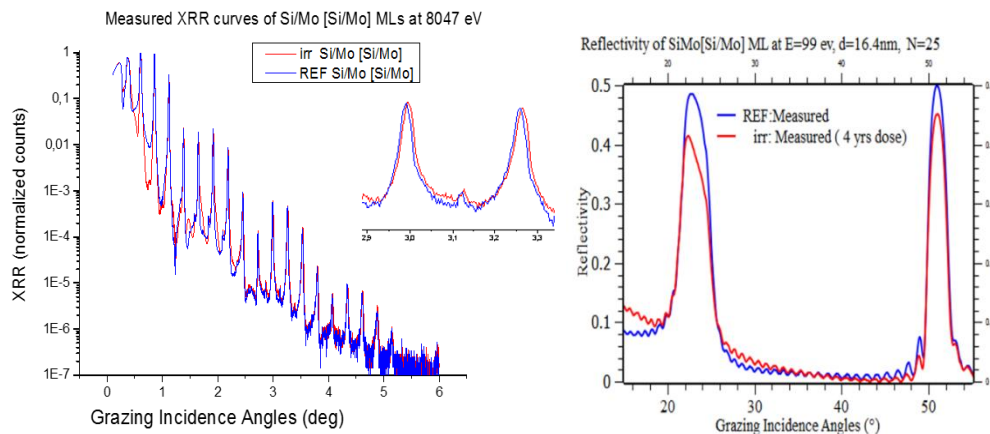


Figure 2: left) Measured XRR plots of REF and irr samples both with capping structure CL1, and on the right) is GI-EUV reflectivity at 99 eV for the same samples. The onset on the left shows a slight shift of Bragg peaks of irr sample with CL1. Note that irr refers to irradiated sample and REF is the non-irradiated sample.

In a similar manner, measured XRR and GI-EUVR curves for MLs with CL2 on the top of the ML structures are given in Fig 3.

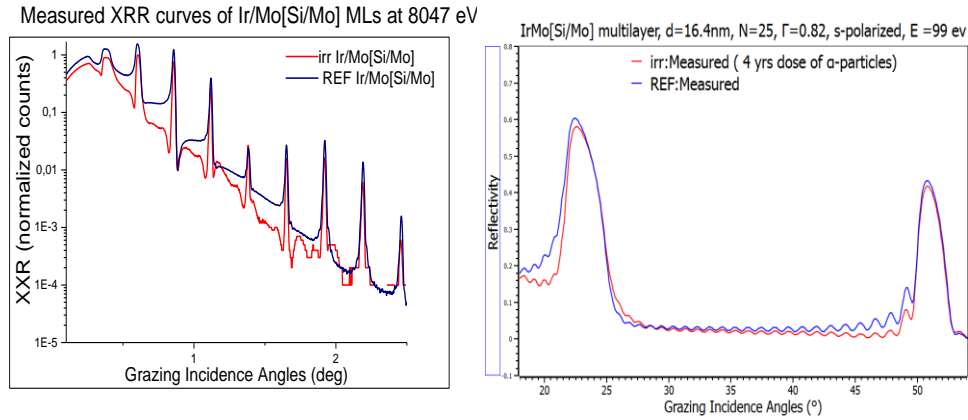


Figure 3: left) Measured XRR plots of REF and irr samples both with capping structures CL2, and on the right) is GI-EUV reflectivity at 99 eV for the same ML samples also with CL2.

Both Figs 2 and 3 shows that Bragg peaks are slightly shifted towards higher angles in both XRR and GI-EUVR measurements. We processed the XRR data using a nonlinear least square curve fitting procedure by using the IMD [20] software using genetic algorithm (GA). Fitting Results clearly show for both samples a shrinkage of average period due to ion exposure, of about 0.3 Å and 0.1 Å respectively for sample CL1 and sample CL2 (Table 2).

Table 2: Nonlinear curve fit results of irr and REF samples. Fitting is performed in IMD software at Cu K_{α} line (1.54 Å) and only thicknesses of Si and Mo layers are used as fitting parameters. An intrinsic roughness of 5 Å is introduced to represent interface irregularities during fitting.

	ML with CL1 (REF)	ML with CL1 (irr)	ML with CL2 (REF)	ML with CL2 (irr)
Period (Å)	163.370	163.073	162.617	162.497
Γ – ratio	0.794	0.801	0.802	0.783

The inspection of Figs 2 and 3 clearly evidences also a decreasing reflectivity performances at grazing incidence measurements after low energy He⁺⁺ (4 keV) implantations into the ML structures. The EUV 2nd order Bragg peak reflectivity decreases from 0.48 to 0.40 and from 0.6 to 0.58 respectively for sample CL1 and sample CL2. This is consistent with near normal reflectivity measurements performed at 30.4 nm and reported in [21] for same MLs. The relative changes in reflectivities due to irradiation are very different for the two samples: CL1 lose more intensity than CL2. This is attributed to the different protection capacity of the capping layers CL1 and CL2 [9].

We stress the fact that Bragg peaks in the GI-EUVR measurement are affected differently (Figs 2 and 3). For example: reflectivity of 2nd and 1st order Bragg peaks of the irradiated sample with CL1 (Fig 2 right) decreased by 12.68% and 6% from the corresponding peaks of the non-irradiated reference sample. Similar effects are observed in CL2 (Fig 3 right) but with much less loss of reflectivity. The GI-EUVR measurement setup is aligned such that incidence beam hits same micro-area as the incidence angle is tuned from low grazing to near normal. In addition, pair of irradiated (irr) and reference (REF) samples were fabricated in the same deposition conditions at same time and preserved in a similar storage. Therefore, the discrepancies shown within same ML can be attributed to the damage history of target layers (MLs) due to irradiation of He⁺ flux of 1.5×10^{11} s⁻¹cm⁻² at 4keV for about 5 hours (Fig 4).

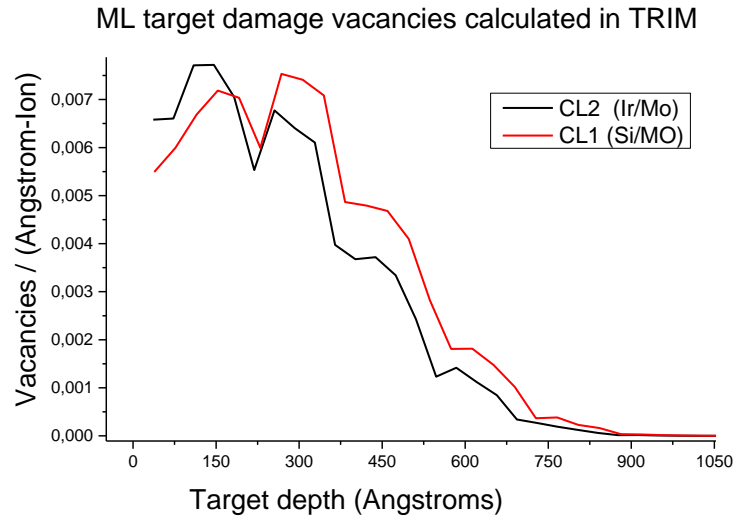


Figure 4: TRIM simulations of low energy He⁺ ions (4 keV) damage vacancies on both CL1 (Si/Mo capping) and CL2 (Ir/Mo capping) MLs. Simulation is performed for a total statistics of 99999 He⁺ ions.

TRIM calculates ion damage events such as number of vacancies, Interstitials, and target atom displacements in the ML structure due to irradiation of energetic ions. However, thermal effects are ignored in TRIM that final damage quantities are likely changed. But still basic damage types occur and useful information can be regained.

In Fig 4, target vacancies refer to empty atomic sites in the ML structures due to displacements by the He⁺ ions as numerically calculated in TRIM. Distribution of damage vacancies throughout the ML structures in both samples might describe the GI-EUV reflectivity pattern in Figs 2 and 3 [22]. Throughout the target depth within the reach of the 4 keV He⁺ ions, ML with CL1 bears more damage vacancies than CL2 (Fig 4). This damage level variation between the two samples, mainly due to different capping structures, explains the relatively greater change of GI-EUVR in Fig 2 (CL1) than the sample in Fig 3 (CL2), both compared to reflectivity performances of respective REF samples. TRIM simulation also clearly demonstrated that damage levels of such low energy He⁺ irradiation concentrates at the top few layers of the ML structures. In addition, damage levels of Si and Mo layers are different. It is then clear that at the top most structures of irradiated MLs, optical contrast ($\Delta\delta$) between Mo and Si layers is affected that in turn decreases the GI-EUVR performances. Apparently, optical damage of upper most layers results in a higher loss of grazing incidence EUV reflectivity than near normal measurements (Figs 2 and 3).

In table 2, nonlinear curve fitting optimization in XRR regime resulted in Γ -ratios significantly different from design value ($\Gamma = 0.82$) for both exposed and non-exposed MLs, and also shows slight variations between reference and exposed samples. Such changes can be associated to the variations of grazing incidence reflectivity particularly also in the EUV wavelength [22, 23] due to the formation of interdiffusion layers [15]. A nonlinear curve fits to measured GI-EUVR data of the four ML samples near the sensitive Si edge energy (99 eV) enables to retrieve optical and structural parameters of each layer (Figure 5). This is such a powerful and innovative method that slight changes in thickness (Δt) and optical properties ($\Delta\delta$) due to the irradiation of He⁺ ions is identified for each layer of the ML structure. Fittings are carried out in the presence of moly-silicide interlayers (Mo_xSi_y) in the capping and interior structures. Since the variation of parameters in the capping structures should not disturb the overall performance of a ML significantly, Figure 5 emphasizes on the accuracy of optical and thickness parameters of the interior layers.

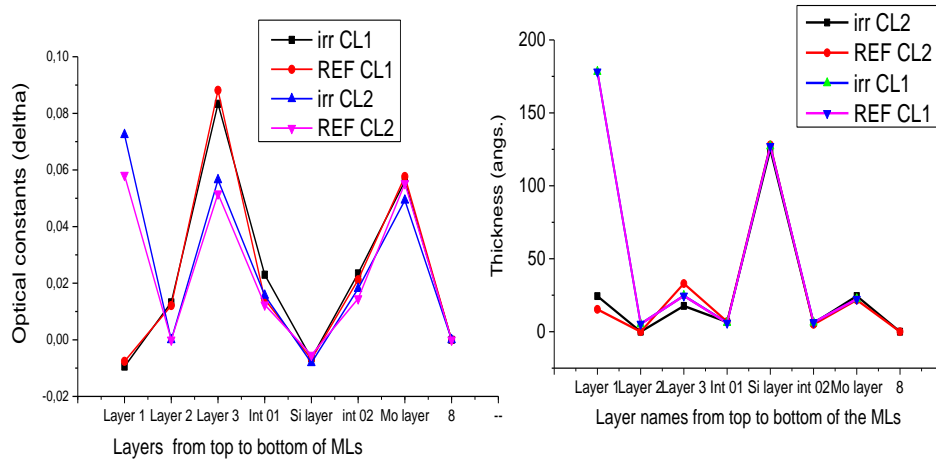


Figure 5: left) Optical constants (δ), and right) layer thicknesses of MLs reconstructed from GI-EUVR curve fits in IMD software using genetic algorithm (GA) optimization. ML structures with interface diffusion regions are design in IMD during fitting. Results show optical constants of layers are more affected by the ion irradiation than thicknesses.

4. SUMMARY

In the current work, four Si/Mo ML samples with CL1 (Si/Mo) and CL2 (Ir/Mo) were originally prepared for METIS coronagraph of SOLO mission. Analysis of impact of low energy He⁺ ions irradiation of the MLs is performed. A novel GI-EUVR measurement near Si edge (99 eV) makes the analysis more innovative and sensitive. With this new method combined with the theoretical damage calculations in TRIM, we are able to confirm the degradation of reflectivity performances of MLs due to irradiations of low energy ions. It is also possible to derive, through a nonlinear curve fit of GI-EUVR measured data, the minor optical changes induced. The optical damage induced are however limited only at the top few layers that causes the 2nd order Bragg peak in Figs 2 and 3 to depreciate more than the Bragg peaks at higher angles. The stability of Ir containing capping structure is found to resist damage events better. Further work on validation with other ML samples will be paramount important.

ACKNOWLEDGEMENT

The writers acknowledge financial support from the EU FP7 Erasmus Mundus Joint Doctorate Programme EXTATIC under framework partnership agreement FPA-2012-0033. This work was also performed under the support of STSM COST Action MP1203. We also thank Dr. Chiara Maurizio from Physics department in Padova for making XRR measurements. Much appreciation to Nardello, M., Zuppella, P., Corso, A. J., and Pelizzo, M. G. for discussions and consultations.

REFERENCES

- [1] K. A. Potocki, M. A. Calabrese, D. Carson, J. Ayon, J. Robinson, J. Oberright, J. T. VanSant, A. Natl Aeronautics Space, and I. Ieee, "NASA's sun-earth connection program strategic planning, missions & technology (2003-2028)," in 2003 Ieee Aerospace Conference Proceedings, Vols 1-8(2003), pp. 4009-4022.
- [2] D. Muller, R. G. Marsden, O. C. St Cyr, and H. R. Gilbert, "Solar Orbiter Exploring the Sun-Heliosphere Connection," *Solar Physics* 285, 25-70 (2013).
- [3] S. R. Cranmer, "Self-Consistent Models of the Solar Wind," *Space Science Reviews* 172, 145-156 (2012).
- [4] M. Miceli, F. Reale, S. Gburek, S. Terzo, M. Barbera, A. Collura, J. Sylwester, M. Kowalinski, P. Podgorski, and M. Gryciuk, "X-ray emitting hot plasma in solar active regions observed by the SphinX spectrometer," *Astronomy & Astrophysics* 544 (2012).

- [5] P. Zuppella, A. J. Corso, P. Nicolosi, D. L. Windt, and M. G. Pelizzo, "Innovative multilayer coatings for space solar physics: performances and stability over time," *Euv and X-Ray Optics: Synergy between Laboratory and Space Ii* 8076 (2011).
- [6] A. J. Corso, P. Zuppella, P. Nicolosi, D. L. Windt, E. Gullikson, and M. G. Pelizzo, "Capped Mo/Si multilayers with improved performance at 30.4 nm for future solar missions," *Optics Express* 19, 13963-13973 (2011).
- [7] J. P. Delaboudiniere, R. A. Stern, A. Maucherat, F. Portier-Fozzani, W. M. Neupert, J. B. Gurman, R. C. Catura, J. R. Lemen, L. Shing, G. E. Artzner, J. Brunaud, A. H. Gabriel, D. J. Michels, J. D. Moses, B. Au, K. P. Dere, R. A. Howard, R. Kreplin, J. M. Defise, C. Jamar, P. Rochus, J. P. Chauvineau, J. P. Marioge, F. Clette, P. Cugnon, and E. L. Van Dessel, "Imaging the solar corona in the EUV," in *Sun and Its Atmosphere*, E. Antonucci, and M. A. Shea, eds. (1997), pp. 2231-2237.
- [8] S. R. Habbal, "Imaging the source regions of the solar wind," in *Robotic Exploration Close to the Sun: Scientific Basis*, S. R. Habbal, ed. (1997), pp. 105-112.
- [9] A. J. Corso, P. Zuppella, P. Nicolosi, and M. G. Pelizzo, "Long term stability of optical coatings in close solar environment," *Solar Physics and Space Weather Instrumentation Iv* 8148 (2011).
- [10] L. Rossi, L. Jacques, J.-P. Halain, E. Renotte, T. Thibert, and D. Grodent, "Space radiation parameters for EUV and the Sun Sensor of Solar Orbiter, ESIO and JUDE instruments," *Modeling, Systems Engineering, and Project Management for Astronomy Vi* 9150 (2014).
- [11] S. Nannarone, F. Borgatti, A. DeLuisa, B. P. Doyle, G. C. Gazzadi, A. Giglia, P. Finetti, N. Mahne, L. Pasquali, M. Pedio, G. Selvaggi, G. Naletto, M. G. Pelizzo, and G. Tondello, "The BEAR beamline at ELETTRA," *AIP Conference Proceedings*, 450-453 (2004).
- [12] M. Oetzel, and G. Heger, "Laboratory X-ray powder diffraction: a comparison of different geometries with special attention to the usage of the CuK alpha doublet," *Journal of Applied Crystallography* 32, 799-807 (1999).
- [13] S. M. Giday, P. Zuppella, M. G. Pelizzo, and P. Nicolosi, "Exploring EUV near absorption edge optical constants for enhanced and sensitive grazing incidence reflectivity," in *Optics for Euv, X-Ray, and Gamma-Ray Astronomy Vi*, S. L. Odell, and G. Pareschi, eds. (2013).
- [14] M. H. Modi, G. S. Lodha, M. Nayak, A. K. Sinha, and R. V. Nandedkar, "Determination of layer structure in Mo/Si multilayers using soft X-ray reflectivity," *Physica B-Condensed Matter* 325, 272-280 (2003).
- [15] S. Roy, and B. N. Dev, "X-ray standing waves in a multi-trilayer system with linearly varying period," *Applied Surface Science* 257, 7566-7572 (2011).
- [16] J. F. Ziegler, M. D. Ziegler, and J. P. Biersack, "SRIM - The stopping and range of ions in matter (2010)," *Nuclear Instruments & Methods in Physics Research Section B-Beam Interactions with Materials and Atoms* 268, 1818-1823 (2010).
- [17] T. S. Kavetsky, J. Borc, Y. Y. Kukhazh, and A. L. Stepanov, "The Influence of Low Dose Ion-Irradiation on the Mechanical Properties of PMMA Probed by Nanoindentation (2015).
- [18] J. E. Butterworth, and C. J. Barton, "TRIMCAT, a TRIM interface for GARFIELD," *Journal of Instrumentation* 4 (2009).
- [19] K. Salamon, O. Milat, N. Radic, P. Dubcek, M. Jercinovic, and S. Bernstorff, "Structure and morphology of magnetron sputtered Wfilms studied by x-ray methods," *Journal of Physics D-Applied Physics* 46 (2013).
- [20] D. L. Windt, "IMD, Version 5, Installation and User's Manual," (2013).
- [21] M. Nardello, P. Zuppella, V. Polito, A. J. Corso, S. Zuccon, and M. G. Pelizzo, "Stability of EUV multilayer coatings to low energy alpha particles bombardment," *Optics Express* 21, 28334-28343 (2013).
- [22] M. Kulik, and J. Zuk, "CORRELATION BETWEEN OPTICAL-PROPERTIES AND NUCLEAR-DAMAGE PROFILES IN ION-IMPLANTED OXIDIZED GAP CRYSTALS," *Nuclear Instruments & Methods in Physics Research Section B-Beam Interactions with Materials and Atoms* 15, 744-747 (1986).
- [23] M. N. a. G. S. Lodha, "Optical Response Near the Soft X-Ray Absorption Edges and Structural Studies of Low Optical Contrast System Using Soft X-Ray Resonant Reflectivity," *Journal of Atomic, Molecular, and Optical Physics* 2011, 23 (2011).
- [24] S. M. Giday, P. Zuppella, M. G. Pelizzo, and P. Nicolosi, "Exploring EUV near absorption edge optical constants for enhanced and sensitive grazing incidence reflectivity," in *Optics for Euv, X-Ray, and Gamma-Ray Astronomy Vi*, S. L. Odell, and G. Pareschi, eds. (2013).
- [25] S. Roy, and B. N. Dev, "Ion-beam-induced mixing in a Si/Co/Si system involving ultrathin layers: A grazing-incidence X-ray standing-wave study," *Physica Status Solidi a-Applications and Materials Science* 209, 1511-1519 (2012).

- [26] G. Boon Tong, N. Siew Kien, Y. Seong Ling, W. Chiow San, D. Chang Fu, and S. A. Rahman, "Structural and optical properties of the nc-Si:H thin films irradiated by high energetic ion beams," *Journal of Non-Crystalline Solids* 363, 13-19 (2013).
- [27] S. A. Nouh, Y. E. Radwan, D. Elfiky, M. M. Abutalib, R. A. Bahareth, T. M. Hegazy, and S. S. Fouad, "Structure, thermal, optical and electrical investigation of the effect of heavy highly energetic ions irradiations in Bayfol DPF 5023 nuclear track detector," *Radiation Physics and Chemistry* 97, 68-74 (2014).